crystals

MDPI

Article

Characterization of Ca-Dicarboxylate Salt Hydrates as Thermochemical Energy Storage Materials

Jakob Werner [1,*], Jakob Smith [1], Berthold Stöger [2], Werner Artner [2], Andreas Werner [3] and Peter Weinberger [1,*]

[1] Institute of Applied Synthetic Chemistry, Getreidemarkt 9/163-01-3, A-1060 Vienna, Austria; jakob.smith@tuwien.ac.at
[2] X-ray Center, Getreidemarkt 9, A-1060 Vienna, Austria; bstoeger@mail.tuwien.ac.at (B.S.); werner.artner@tuwien.ac.at (W.A.)
[3] Institute of Energy Systems and Thermodynamics, Getreidemarkt 9/302, A-1060 Vienna, Austria; andreas.werner@tuwien.ac.at
* Correspondence: jakob.werner@tuwien.ac.at (J.W.); peter.e163.weinberger@tuwien.ac.at (P.W.)

Abstract: Salt hydrates are highly promising materials for thermochemical energy storage applications to store waste heat below 200 °C. Although highly researched and theoretically promising, in practical applications salt hydrates often cannot fulfill expectations. Based on the promising results of the Ca-oxalate monohydrate/Ca-oxalate system, other Ca-dicarboxylate salt hydrates were investigated to determine whether potential materials for heat storage can be found amongst them. A simultaneous thermal analysis showed that all candidates are applicable in the temperature range of 100–200 °C, and thermally stable up to 220 °C. Calcium malonate dihydrate (637 J/g), calcium terephthalate trihydrate (695 J/g), and tetrafluoro calcium terephthalate tetrahydrate (657 J/g) have shown higher enthalpies of dehydration than Ca-oxalate monohydrate. Due to the investigation of derivatives of Ca-terephthalate, it is possible to report the crystal structure of 2-fluoro calcium terephthalate. In single crystals, it forms a trihydrate and crystallizes in the Pmna space group ($Z = 4$, $Z' = \frac{1}{2}$) forming infinite chains of Ca atoms. De- and rehydration reactions of the most promising candidates were studied in situ with powder X-ray diffraction showing the structural changes between the hydrate and anhydrate states.

Keywords: thermochemical storage materials; thermochemical and thermophysical material properties; crystallization; crystal structure

Citation: Werner, J.; Smith, J.; Stöger, B.; Artner, W.; Werner, A.; Weinberger, P. Characterization of Ca-Dicarboxylate Salt Hydrates as Thermochemical Energy Storage Materials. *Crystals* **2023**, *13*, 1518. https://doi.org/10.3390/cryst13101518

Academic Editors: S. Afflerbach and Reinhard Trettin

Received: 29 September 2023
Revised: 16 October 2023
Accepted: 18 October 2023
Published: 19 October 2023

1. Introduction

Increasing energy efficiency is a fundamental need in order to tackle climate change, reduce greenhouse gas emissions, and achieve energy independence. According to the International Energy Agency (IEA), the production of heat is accountable for around 50% of the global demand of primary energy [1,2]. A significant part of the heat produced is subsequently lost as low-grade waste heat and released into the environment [3]. In 2021, the global demand of primary energy was 595.15 EJ, 82% being covered by fossil fuel sources [4]. Considering that heat production is the biggest "end-use" of primary energy, these numbers highlight the enormous storage potential [5–7]. Thermochemical energy storage (TCES) systems are a promising technique for thermal heat storage, suitable for a broad range of waste heat recovery applications [8,9]. Salt hydrates are considered to be promising candidates as thermochemical materials (TCMs) for storing heat in the temperature range of 100–200 °C and have been extensively researched [8,10–12]. In general, salt hydrates can obtain high storage densities, often coming from high latent heat capacities, which also enables the application of salt hydrates as phase change materials (PCMs) in latent heat storage systems [13–15].

A TCES system that relies on salt hydrates as TCMs uses a reversible chemical reaction as storage principle. Equation (1) illustrates a general reaction of an anhydrous salt *A* with *n* moles of water to react to its corresponding hydrate under the release of a certain heat of reaction $\Delta_r H$ [16,17]. Figure 1 displays a graphical illustration of the storage principle. For a technically promising TCES system, parameters like high energy densities, high cycle stability, usage of non-toxic, low-cost, and non-corrosive materials, as well as fast reaction times, are key [18,19].

$$A + n\ H_2O \rightleftharpoons A \cdot nH_2O + \Delta_r H, \quad (1)$$

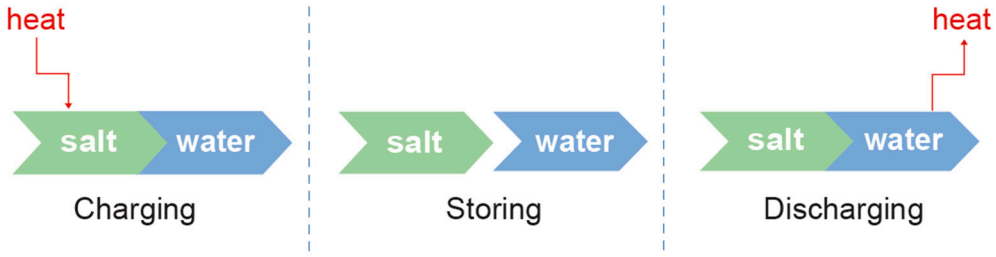

Figure 1. Storage principle of a TCES system utilizing salt hydrates as TCMs.

A systematic search algorithm screening for chemical reactions suitable to become part of a thermal energy storage system proposed the calcium oxalate monohydrate/calcium oxalate ($CaC_2O_4 \cdot H_2O/CaC_2O_4$) system as such a potential reaction [20]. The material was analyzed and subsequently characterized, confirming the theoretically promising data by showing excellent cycle stability, full reversibility of reaction, and tuneability of the storage temperature via varying the water vapor concentration [21,22]. Based on the data for the $CaC_2O_4 \cdot H_2O/CaC_2O_4$ system, a small library of calcium dicarboxylate salt hydrates (**1**–**5f**) was chosen to conduct the study of these calcium salt hydrates to investigate whether some of the candidates share the strengths of the oxalate or can even outperform it. The investigated candidates are displayed in Figure 2, and the compound names are found in Table 1.

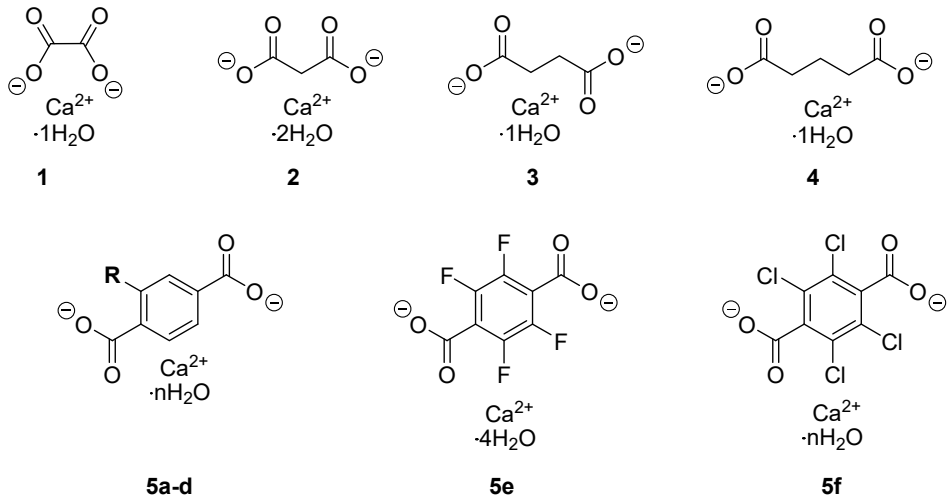

Figure 2. Overview of the investigated Ca-dicarboxylate salt hydrates.

The thermal behavior of Ca-malonate dihydrate has been investigated before [23,24], and so too has the behavior of its coordinated water [25]. Ca-succinate is reported to form a trihydrate in single crystals [26,27]. For Ca-succinate monohydrate, as well as Ca-glutarate monohydrate, an existing, detailed thermal analysis is unknown to the authors. Ca-terephthalate is a valuable precursor for building metal organic frameworks (MOFs) as

well as being the subject of research in macromolecular chemistry [28–33]. It possesses a crystal structure documented in the literature [34].

Table 1. Compound names of investigated Ca-dicarboxylate salt hydrates.

Compound Number	Compound Name
1	Calcium oxalate monohydrate
2	Calcium malonate dihydrate
3	Calcium succinate monohydrate
4	Calcium glutarate monohydrate
5a (R=H)	Calcium terephthalate trihydrate
5b (R=CH_3)	2-methyl calcium terephthalate n-hydrate
5c (R=F)	2-fluoro calcium terephthalate trihydrate
5d (R=Cl)	2-chloro calcium terephthalate trihydrate
5e	Tetrafluoro calcium terephthalate tetrahydrate
5f	Tetrachloro calcium terephthalate n-hydrate

Despite the existing characterizations, to the best of the authors' knowledge, the mentioned salt hydrates have not been investigated as potential thermochemical materials for TCES systems. However, despite the high potential shown by the $CaC_2O_4 \cdot H_2O/CaC_2O_4$ system, the family of calcium dicarboxylate salt hydrates is also suitable to study the influence of various chemical factors on the thermophysical properties of the TCMs. In the past, promising salt hydrates were scrutinized, in an attempt to unveil all their properties related to a TCM application. Prominent examples are $CaCl_2$ [35,36], $MgSO_4$ [37–40], and $SrCl_2$ [41,42]. In this paper, the chemical nature of the compounds and its influence on the thermophysical properties shall be considered. For this purpose, derivatives of Ca-terephthalate were prepared and investigated. By inserting functionalizations with different electronic properties into the system, it is interesting to follow their influence on properties like the onset temperatures of dehydration or the enthalpy of dehydration.

2. Materials and Methods

2.1. Materials

Calcium oxalate monohydrate (CAS 5794-28-5) was obtained from Sigma-Aldrich (Merck KGaA, Darmstadt, Germany) and used as supplied. Calcium malonate was prepared from malonic acid and calcium carbonate. Calcium carbonate (CAS 471-34-1) was obtained from PanReac AppliChem (Ottoweg 4D-64291 Darmstadt, Germany), and malonic acid (CAS 141-82-2) from fluorochem (14 Graphite Way, Hadfield, Glossop SK13 1QH, UK); both were used without further purification. Calcium succinate (CAS 140-99-8) was purchased from Szabo-Scandic HandelsgmbH (Quellenstraße 110, 1100 Vienna, Austria) and used as supplied. Calcium glutarate monohydrate, as well as calcium terephthalate (CAS 16130-76-0) and its derivatives, were synthesized, and the synthetic procedures are found in the supporting information.

2.2. Synthesis

The exact synthetic protocols are given in Chapter I of the supporting information. Calcium malonate dihydrate was prepared according to the procedure found in the literature [24], i.e., by reaction of malonic acid with calcium carbonate in distilled water. After completed CO_2 formation, a white precipitate was observed, which could be isolated as product.

Ca-glutarate monohydrate, as well as Ca-terephthalate trihydrate and all of its derivatives, were synthesized by mechanochemical means following the proposed procedure for Ca-terephthalate trihydrate preparation found in [43]. In this method, terephthalic acid, $Ca(OH)_2$, and 130 µL H_2O are filled in a ball and milled for 4 h (Reaction (2)).

$$C_8H_6O_4 + Ca(OH)_2 + H_2O \rightarrow CaC_8H_6O_4 \cdot 3H_2O \quad (2)$$

The synthesis of the mono-functionalized Ca-terephthalates was carried out in two steps. In a first step, the mono-functionalized terephthalate was prepared. In a second step, the corresponding calcium salt hydrate was formed by mechanochemical means (see Figure 3).

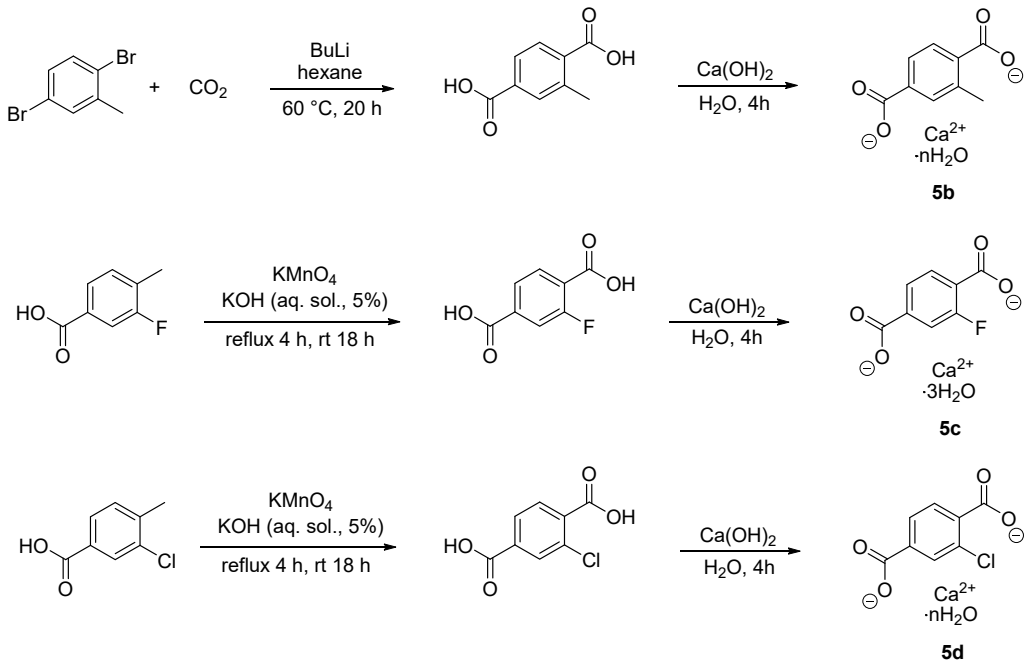

Figure 3. Synthesis of the mono-functionalized Ca-terephthalate hydrates.

2.3. Single Crystal Growth

Crystals of 2-fluoro Ca-terephthalate trihydrate were grown by in situ formation of the target compound and slow evaporation. 2-fluoro Ca-terephthalate is insoluble in water, requiring that it is transformed into the corresponding disodium salt which is water-soluble. The preparation is shown by Reaction (3). The exact synthetic details are found in the supporting information.

$$C_8H_5O_4F + 2\ NaOH \rightarrow Na_2C_8H_6O_4F + 2\ H_2O \quad (3)$$

An aqueous solution of $CaCl_2$ (6.3 mg, 0.05 mmol) was carefully added to a solution of 2-fluoro terephthalic acid disodium salt (10.5 mg; 0.05 mmol) resulting in a slight turbidity. After two weeks of crystallization at room temperature, red single crystals were obtained in a quality suitable for single crystal XRD (Reaction (4)).

$$Na_2C_8H_6O_4F + CaCl_2 + 3\ H_2O \rightarrow CaC_8H_5O_4F{\cdot}3H_2O + 2\ NaCl \quad (4)$$

2.4. Thermal Analysis

The thermal characterization measurements were carried out on a Netzsch STA 449 F1 Jupiter® system equipped with an automatic sample changer and a combined TGA–DSC sample holder. The sample was measured in aluminum crucibles, containing sample masses between 10 and 12 mg at a heating rate of 2 °C/min.

2.5. Powder X-ray Diffraction

The powder X-ray diffraction measurements were carried out on a PANalytical X'Pert Pro diffractometer in Bragg-Brentano geometry, using a mirror for the separation of Cu-K$\alpha_{1,2}$ radiation and a X'Celerator linear detector. The collected diffractograms were evaluated with the PANalytical program suite HighScore Plus v5.1.

For the in-situ monitoring of the experiments, an Anton-Paar XRK 900 reaction chamber was used. The sample was mounted on a hollow ceramic powder sample holder. Dehydration measurements were performed in an atmosphere of dry N_2, with a flow rate set to 0.4 L/min.

2.6. Single-Crystal X-ray Diffraction

X-ray diffraction data of 2-fluoro Ca-terephthalate (CSD 2298055) were collected at T = 100 K in a dry stream of nitrogen on a STOE STADIVARI diffractometer system equipped with a Dectris Eiger CdTe hybrid photon counting detector using Cu-Kα radiation (λ = 1.54186 Å). Data were reduced to intensity values with X-Area, and an absorption correction was applied with the multi-scan approach implemented in LANA [44]. The crystal structure was solved by the dual-space approach implemented in SHELXT [45], and refined against F^2 with JANA [46]. Non-H atoms were refined with anisotropic atomic displacement parameters (ADPs). H atoms connected to C were placed in calculated positions and refined as riding on the parent atom. The water H atoms were refined freely. The F atom was refined as disordered about three crystallographically distinct positions with the sum of the occupancies constrained to 1. The additional difference electron density in parts of the structure suggested an alternative orientation of the inorganic part of the structure. The Ca atoms and water molecules were, therefore, refined as positionally disordered. The ADPs of the minor positions were constrained to those of the major positions up to the pseudo-symmetry relating the orientations (reflection at y = $\frac{1}{4}$). Likewise, the coordinates of the H atoms of the minor positions were connected to those of the major position up to this reflection. Molecular graphics were generated with the program MERCURY [47].

2.7. Scanning Electron Microscopy

SEM images were taken on a FEI Quanta 200 F using a Schottky-FEG Emitter. The measurements were performed with an acceleration voltage of 5 kV and a working distance of 6.4–7.7 mm.

3. Results and Discussion

3.1. Synthesis

The mechanochemical synthesis method described in [43] was a very important procedure to prepare most of the investigated salt hydrates. At first, it was interesting to determine whether it is also applicable to calcium salts with anions different than the terephthalate. For this reason, Ca-oxalate monohydrate was prepared analogously and compared with a purchased sample. For the preparation, oxalic acid (0.55 g, 6.11 mmol) and calcium hydroxide (0.45 g, 6.11 mmol) were filled in a ball mill, 130 µL of deionized water was added, and the mixture was milled for 4 h. The product was obtained as white powder (802 mg, 5.49 mmol, 89 %). The product formation was confirmed with PXRD and IR-spectroscopy (Figure 4), showing the identity of the two compounds.

3.2. Characterization and Thermal Dehydration Experiments

Combined TG-DSC experiments are a well-established method to characterize potential TCMs. The dehydration process of $CaC_2O_4 \cdot H_2O$ is well documented in the literature [21,48] and used as standard for mass-loss calibration in TG analysis [49].

The thermal characterization of the compounds was carried out to determine the applicability of the investigated candidates as thermal energy storage materials in the temperature range from 100 to 200 °C. Decomposition reactions, as well as thermal stability measurements, were not the target of this investigation. Table 2 shows the measured onset temperatures of dehydration (in °C) and enthalpies of dehydration (in J/g) for the investigated calcium dicarboxylate salt hydrates. The two chlorinated derivatives of Ca-terephthalate (**5d** and **5f**) showed a significantly different dehydration behavior than the other components and are, therefore, excluded from the table.

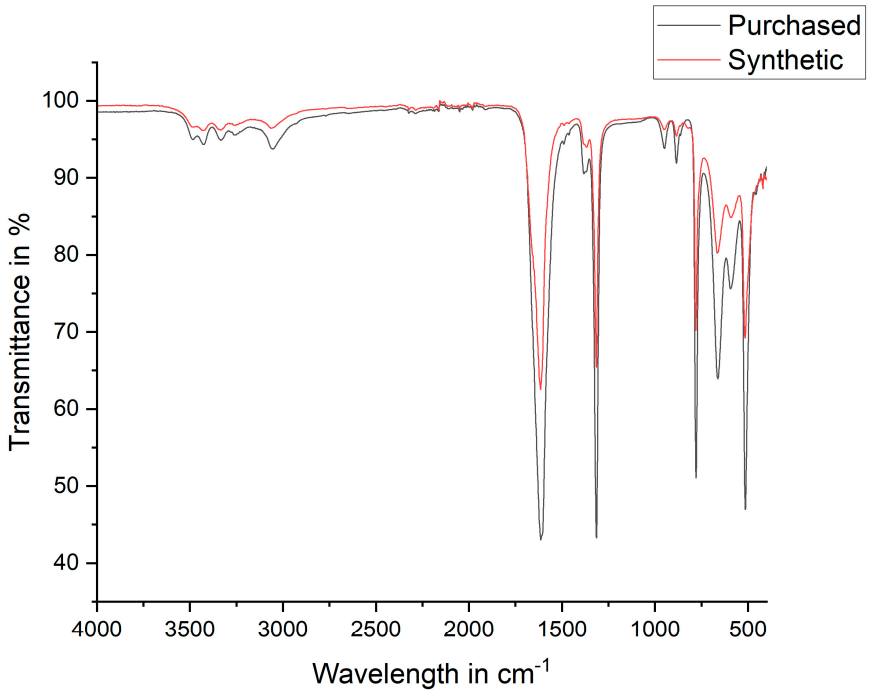

Figure 4. IR spectra of purchased (black) and synthetic (red) Ca-oxalate monohydrate.

Table 2. Onset temperatures of dehydration and measured dehydration enthalpies.

Substance	Theoretical Mass Loss in %	Observed Mass Loss in %	Onset Temperature of Dehydration in °C	ΔH_{deh} in J/g
Ca-oxalate monohydrate	12.3	12.2	156	489
Ca-malonate dihydrate	20.2	17.9	127	637
Ca-succinate monohydrate	10.3	10.2	166	314
Ca-glutarate monohydrate	9.6	12.5	145	418
Ca-terephthalate trihydrate	20.9	20.1	104	695
2-methyl Ca-terephthalate n-hydrate	15.7	15.8	93	220
2-fluoro Ca-terephthalate trihydrate	19.5	15.6	126	483
Tetrafluoro Ca-terephthalate tetrahydrate	19.2	19.2	99	657

Firstly, it should be noted that all included salt hydrates are stable up to 220 °C and possess onset temperatures of dehydration in the desired temperature range from 100 to 200 °C, with **5b** and **5e** being slightly below. Furthermore, none of the candidates showed melting or deliquescence effects throughout all experimental investigations. Three candidates (**2**, **5a**, **5e**) achieved higher enthalpies of dehydration than calcium oxalate monohydrate. Ca-malonate dihydrate (**2**), Ca-terephthalate trihydrate (**5a**), and Tetrafluoro Ca-terephthalate tetrahydrate (**5e**) formed higher hydrates (more than one water per formula unit). Figure 5 shows the STA curves for calcium malonate dihydrate (**2**), and Figure 6 shows the TG and DSC curves for calcium terephthalate (**5a**), in which the TG signal shows a stepless mass loss of 20.1% which corresponds to a loss of 2.85 moles of hydrate water. The enthalpy of dehydration is 695 J/g. The results are in good agreement with literature data [43]. All other STA curves are included in the supporting information (Supplementary Figures S1–S9).

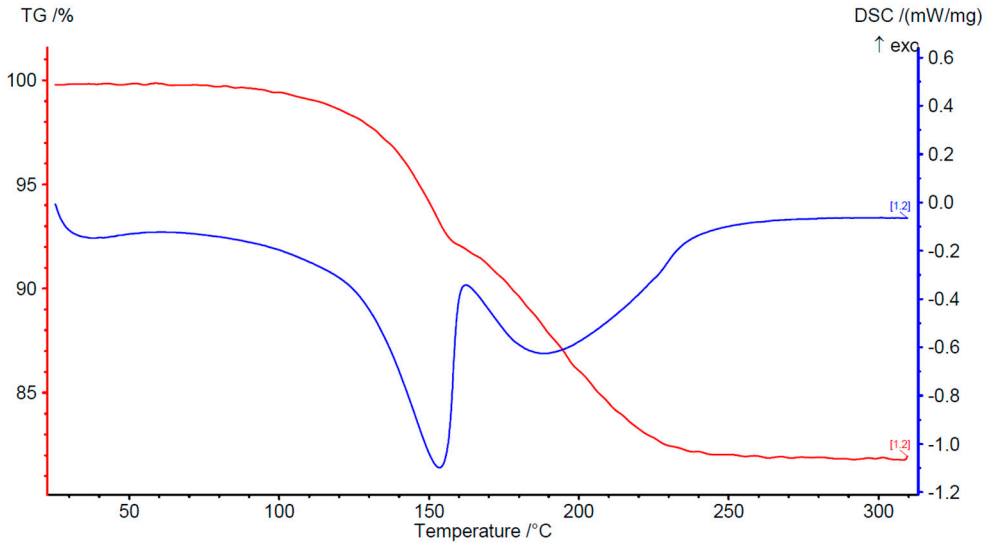

Figure 5. STA curves of **2**.

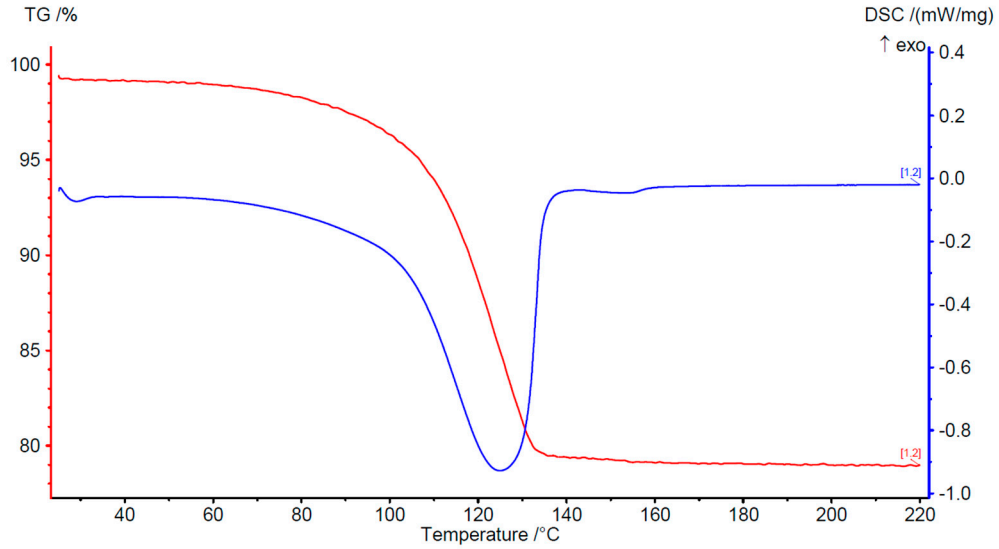

Figure 6. STA curves of **5a**.

The corresponding enthalpies of dehydration $\Delta_{deh}H$ in J/g were converted to J/mol giving the molar dehydration enthalpies $\Delta_{deh}h$. They describe the thermal energy related to the process of dehydration related to the moles of TCM. It consists of two energetic contributions: one necessary to induce a phase change of water, represented by the enthalpy of evaporation $\Delta_e h$, and another necessary for breaking chemical bonds (Δh_{net}) [50]. Equation (5) leads to the net storage enthalpy representing the sole contribution of the TCM to the enthalpy of dehydration. Equation (6) shows that the energy required to evaporate the coordinated water is built up by two parts. $\Delta_v h$ represents the latent part, which is the energy necessary to evaporate the water. The other part represents the amount of sensible heat stored in the process of heating the water from a storage temperature T_1 to a desired evaporation temperature T_2. In the case of both storage and evaporation at room temperature ($T_1 = T_2 = 25$ °C), the enthalpy values obtained are found in Table 3 (Δh_{net_25}), and the calculations are based on the methodology of [42,50].

$$\Delta h_{net} = \Delta_{deh}h - n \cdot \Delta_e h, \quad (5)$$

$$\Delta_e h = \Delta_v h + \int_{T_1}^{T_2} c_p dT, \quad (6)$$

Table 3. Calculated enthalpies for investigated calcium dicarboxylic acid hydrates.

TCM	Moles of Crystal Water	Moles of Water Lost in TGA	$\Delta_{deh}h$	$\Delta_{deh}h/n$ H_2O	Δh_{net_25}
			kJ/mol	kJ/mol H_2O	kJ/mol
1	1	0.99	71.33	72.20	27.87
2	2	1.72	110.26	64.10	34.59
3	1	0.98	54.60	55.46	11.29
4	1	1.35	81.36	60.29	21.99
5a	3	2.85	177.52	62.26	52.09
5c	3 *	2.29	127.73	34.65	27.00
5e	4	3.65	224.66	61.55	64.10

* determined by single-crystal analysis.

The net enthalpy values show that in the cases of Ca-malonate dihydrate (**2**), Ca-terephthalate trihydrate (**5a**), and its tetrafluorinated derivative (**5e**) the higher enthalpy of dehydration is not only achieved by an enhanced number of crystal water molecules. For the named candidates, the energetic contribution of the material itself is higher than in the case of Ca-oxalate monohydrate, since Δh_{net} directly corresponds to the actual energy storage potential [50]. The TG analysis of the monofluorinated compound (**5c**) gave a mass loss of 2.29 moles of crystal water. Since the crystal structure was not known to the literature, the determination of the exact structural properties was desirable, also to clarify the bonding situation of the crystal water.

3.3. Structure Description of 2-Fluoro Ca-Terephthalate Trihydrate

The crystal structure of 2-fluoro Ca-terephthalate trihydrate (*Pmna*, $Z = 4$, $Z' = \frac{1}{2}$) is built of infinite chains of Ca atoms located on the *m* [100] reflection plane and connected by 2-fluoroterephthalate ions and water molecules extending in the [100] direction (Figure 7, top). A bridging water molecule located on a 2 [010] rotation axis connects two adjacent Ca atoms in these chains. Two further water molecules, located on *m* [100], complete the coordination sphere of the Ca atom. The infinite chains are connected by hydrogen bonds from the water molecules to the non-coordinating carboxylate group, forming a triperiodic network (Figure 7, bottom).

The monofluorinated-*para*-phenylene moiety is disordered around the *m* [100] reflection plane of the *Pmna* space group (Figure 8). The F atom is additionally disordered and could be located at three out of the four crystallographic C atom positions. The major F1 position (30.2 (5)% occupancy) is located on the side of the uncoordinated carboxylate group. The alternative F1′ position on the same side features 3.7 (7)% occupancy. Finally, on the side of the coordinating carboxylate group, F2 is occupied by 16.1 (4)%. It should be noted that the occupancies amount to 0.5 owing to the disorder of the phenylene moiety around the *m* 100 reflection plane. Given the occupancy ratio of ca. 7.5:1 for the F1/F1′ pair, one could expect a F2′ atom at the fourth position with ca. 2% occupancy, which is, however, below the detection limit of a routine X-ray structure analysis.

The structure of **5c** features a polytype character as evidenced by distinct one-dimensional diffuse scattering along **c***, which means that the structure is ordered on the (001) plane but features a pronounced stacking-fault probability. The alternative arrangements of the layers are reflected by 'phantom atoms' corresponding to a reflection of the Ca^{2+} ions and water molecules on the $y = \frac{1}{4}$ plane, with 4.5% occupancy. This implies an order-disorder (OD) theory [51] interpretation of the polytypism as follows: The structure is built of two kinds of layers extending on the (001) plane. Layers of the first kind are built of the terephthalate ions. Owing to the disorder of the phenylene moieties, but ignoring the occupancies of the F

atoms, these layers possess a pseudo-reflection plane at $y = \frac{1}{4}$. The second kind of layer (Ca^{2+} ions and water molecules) does not possess such a reflection symmetry and can, therefore, appear in two orientations with respect to this reflection plane. This second orientation explains the 'phantom atoms'. There is an infinite number of possible polytypes, depending on the sequence of the orientation of these layers. Nevertheless, all these polytypes are locally equivalent and, therefore, energetically very similar.

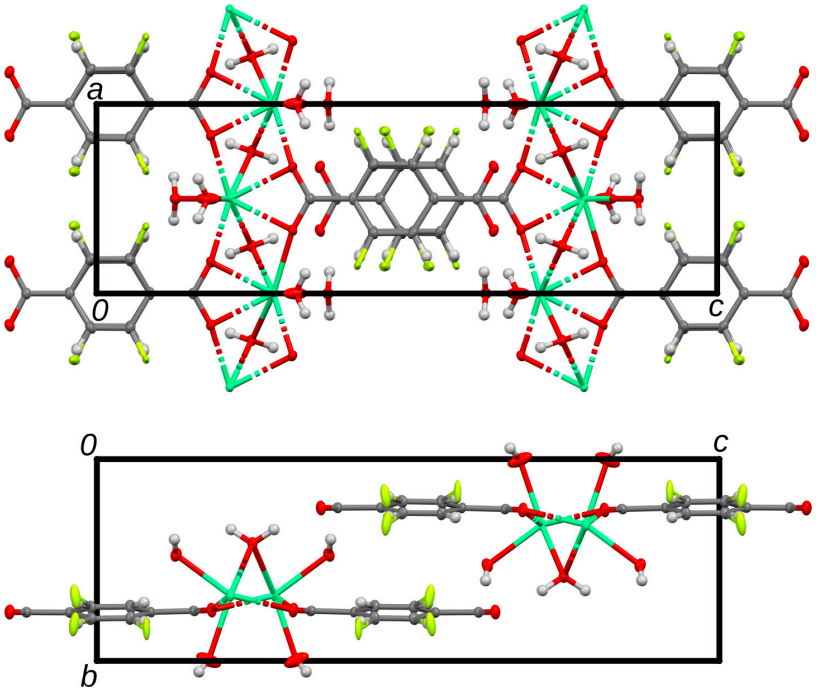

Figure 7. Crystal structure of 2-fluoro calcium terephthalate viewed along (**top**) [010] and (**bottom**) [100]. Ca (green), F (yellow), O (red), and C (grey) atoms are represented by ellipsoids drawn at the 50% probability levels; H atoms are represented by spheres of arbitrary radius.

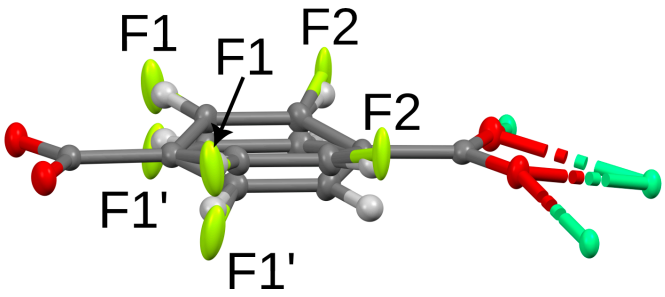

Figure 8. The mono-F-terephthalate molecule and coordinating Ca atoms. Colors as in Figure 7.

The structures of **5c** and the unfluorinated analogue (**5a**) [34] are closely related. In fact, both are built of the same kind of infinite chains connected by an analogous hydrogen bond network. However, in the unfluorinated analogue, the phenylene moieties are not disordered around a reflection plane, which leads to a symmetry descent of order 2 to $P2_1/c$ (permutation of the *b* and *c* axes). The reduction from orthorhombic to monoclinic symmetry leads to a pronounced deviation from the orthorhombic metrics, with a reported β angle of 92.3°. Attempts to refine 2-fluoro Ca-terephthalate trihydrate in the $P2_1/c$ space group, with twinning by the lost point operations, did not resolve the disorder of the phenylene moieties and showed distinct signs of overparameterization, namely, a large correlation of ADPs and highly anisotropic ADPs.

3.4. In Situ De- and Rehydration

Due to the unavailability of a suitable STA setup for rehydration, an in situ PXRD approach was used to study the de- and rehydration reactions in as detailed a manner as possible. Due to the promising enthalpy data from the TGA-DSC measurements, candidates **2**, **5a**, **5c** and **5e** were selected for the in situ PXRD measurements. The dehydration was caried out at isothermal conditions with a chosen temperature $T_{deh} = T_{onset} + 10$ °C. T_{onset} corresponds to the onset temperature of dehydration observed in the STA experiments.

The rehydration was carried out with hot water vapor pumped into the system with a HPLC pump. Under the chosen conditions, all four salt hydrates were effortlessly de- and rehydratable.

The two images, a and b, in Figure 9 show the collected diffraction patterns for the calcium terephthalate trihydrate/calcium terephthalate system. Under the applied conditions, rehydration happens too fast to monitor intermediate structures with a scan of 5°–60° 2θ. The third rehydration (blue curve in Figure 9b) shows a reflection at 21.6937 °2θ remaining from the anhydrate structure. The measurement setup can cause inevitable material loss, mainly because of an abrupt exposition to the N_2 stream. After the 3rd cycle, the remaining amount of sample was too low to perform a 4th cycle. With this limitation it was not possible to confirm whether the reflection at 21.6937 °2θ means that a part of the material is no longer rehydratable after three cycles. However, in SEM images (Figure 10) no visible particle degradation was observed, indicating that 5a is cyclable for >3 cycles and the observed anhydrate reflection derives from the PXRD setup. To prove that the diffraction pattern of the anhydrate is obtained from fully dehydrated Ca-terephthalate, an IR-spectrum was recorded (Figure 11).

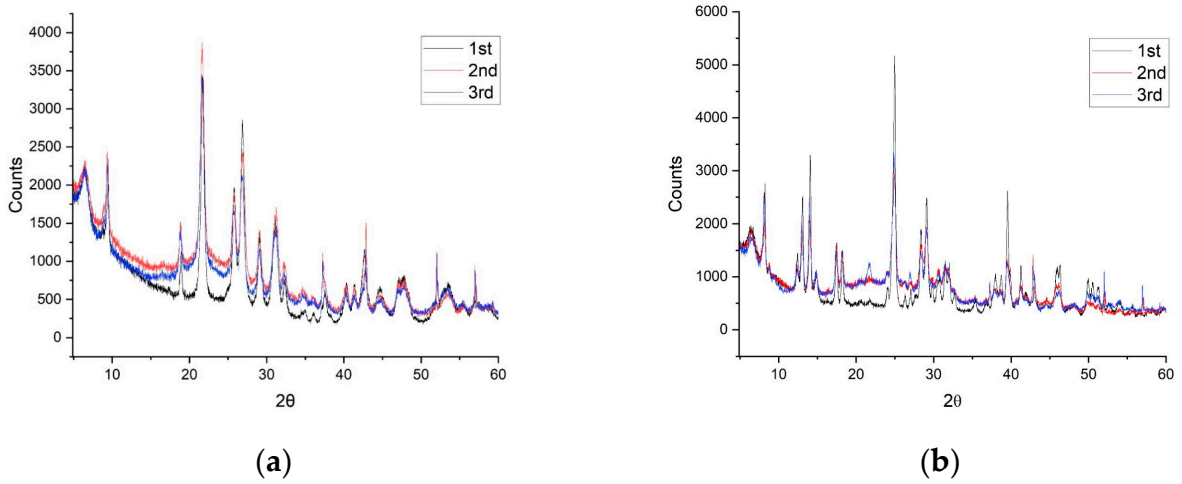

Figure 9. (**a**) Diffraction patterns after three dehydration cycles of **5a** and (**b**) after the corresponding rehydration reactions.

The red curve in Figure 11 shows a prominent, broad absorption band at 3600–2900 cm^{-1} coming from the OH stretching vibrations of the bound water molecules. The broadening is an effect of H-bonds. In the spectrum of anhydrous **5a**, no bands occur in this region, confirming a full dehydration of the sample.

Figures 12 and 13 show one de- and rehydration cycle of the fluorinated derivatives of calcium terephthalate (**5c** and **5e**). The diffraction patterns in (a) in both figures show a successful rehydration of both compounds, with the anhydrous diffraction pattern in (b).

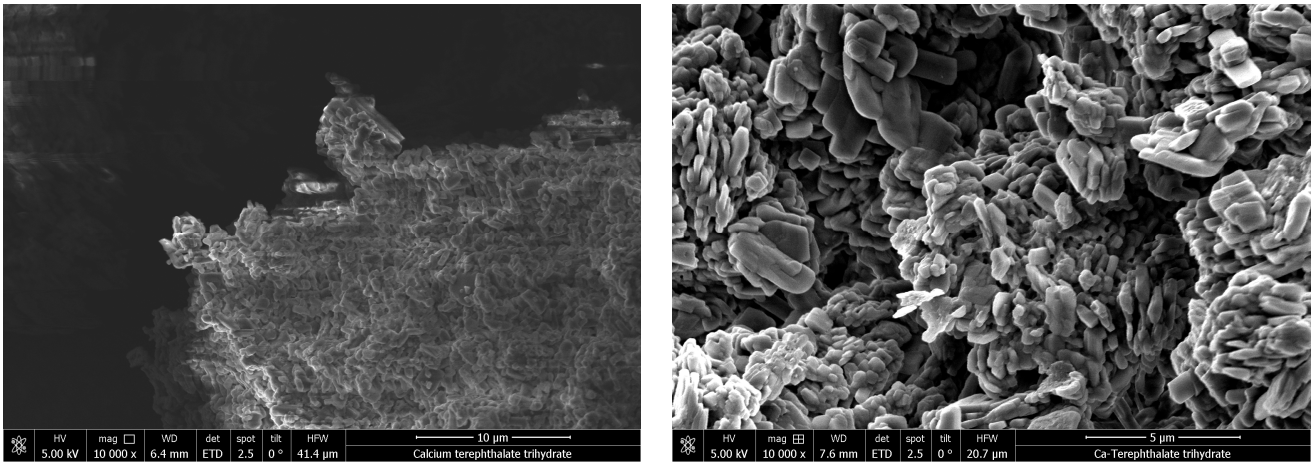

(**a**) (**b**)

Figure 10. SEM pictures of Ca-terephthalate trihydrate after preparation (**a**) and Ca-terephthalate trihydrate after three cycles (**b**) at a magnification of 10,000×.

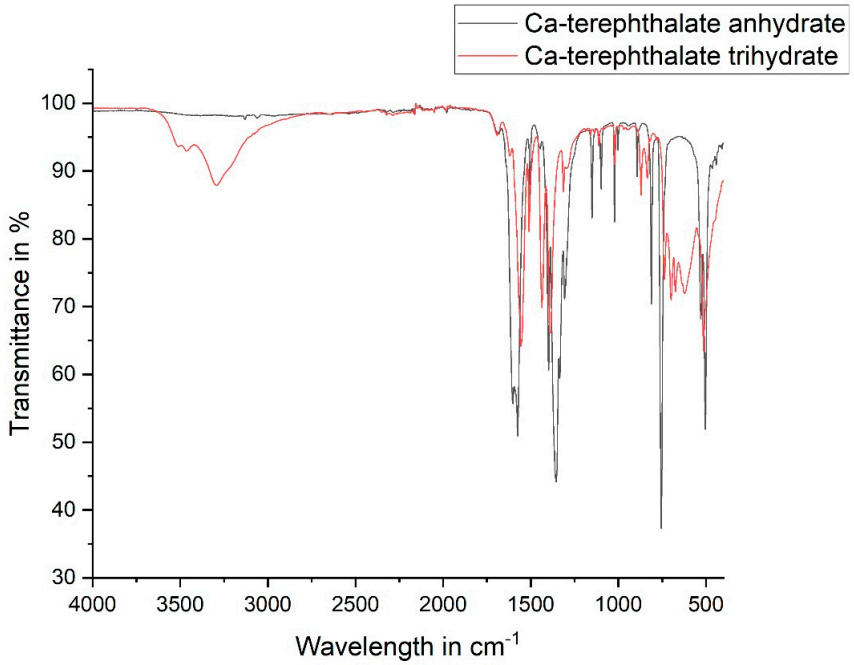

Figure 11. IR-spectra of Ca-terephthalate trihydrate (red) and Ca-terephthalate anhydrate (black).

Due to a high amount of particle movement in the scanning electron microscope, SEM images of **5c** could not be provided in an appropriate quality. Figure 14 shows SEM images for **5e** after preparation (a) and after a full cycle of measurement (b). The rehydrated image is highly comparable to the rehydrated form of **5a** (Figure 10b). In general, the de- and rehydration reactions were monitorable with the applied methodology, making it possible to collect diffraction patterns of the fully hydrated and anhydrous states of the salts **2**, **5a**, **5c**, and **5d**. The corresponding IR spectra of both fully hydrated and anhydrous states are included in the supporting information (Supplementary Figures S24–S29).

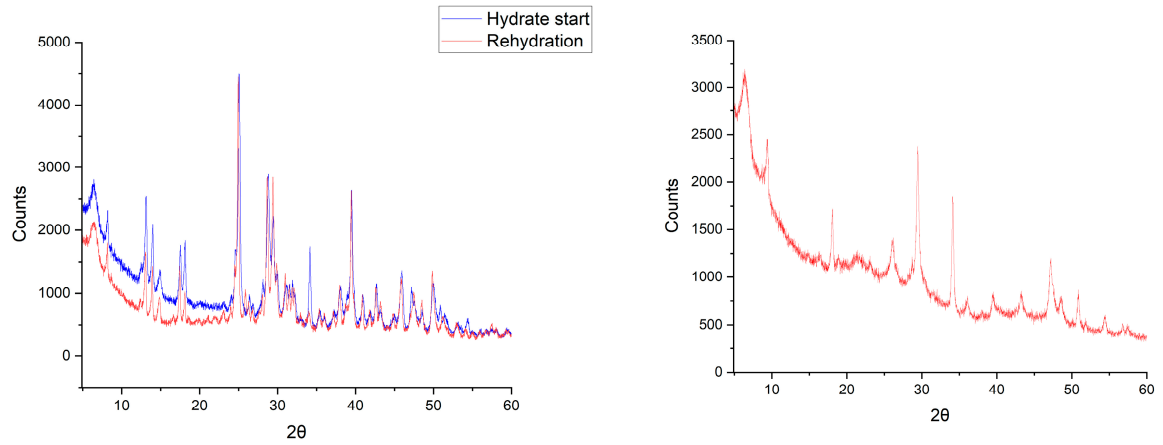

(**a**) (**b**)

Figure 12. Diffraction patterns of (**a**) hydrated and rehydrated **5c**, and (**b**) anhydrous **5c**.

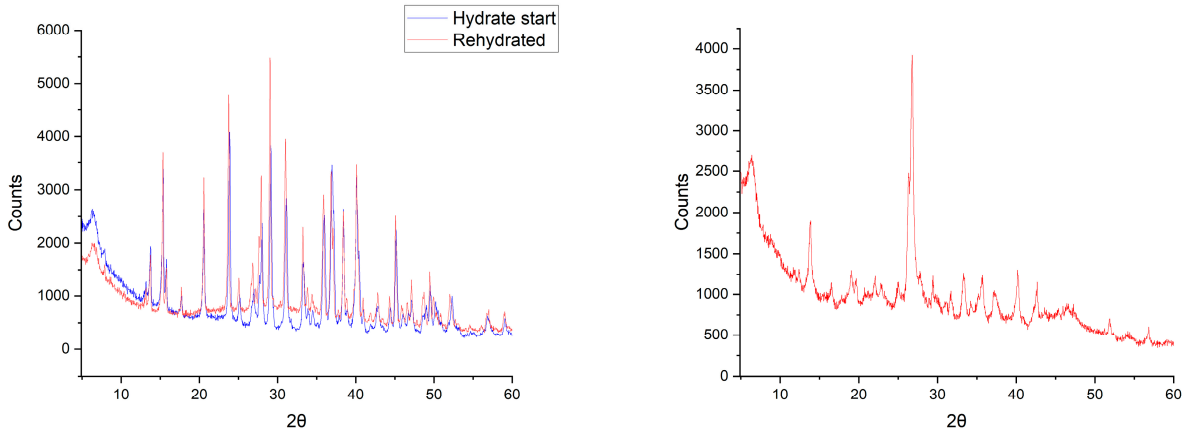

(**a**) (**b**)

Figure 13. Diffraction patterns of (**a**) hydrated and rehydrated **5e**, and (**b**) anhydrous **5e**.

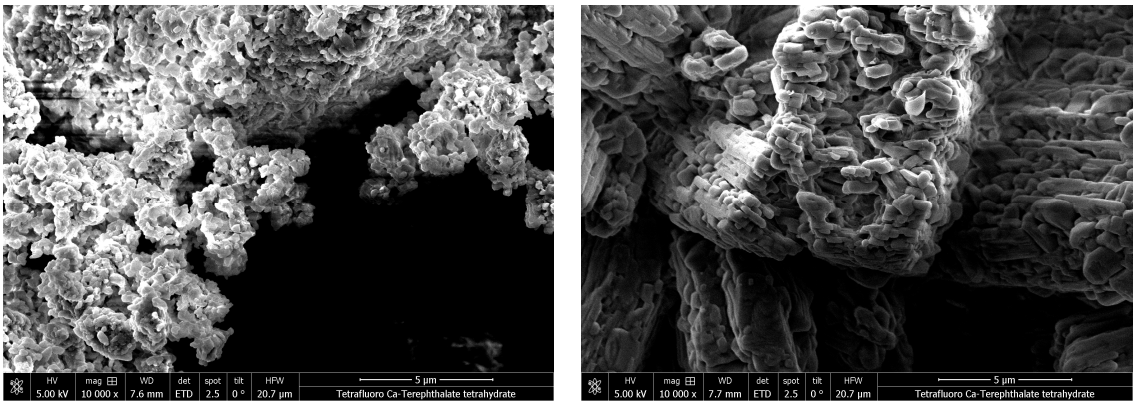

(**a**) (**b**)

Figure 14. SEM pictures of Tetrafluoro Ca-terephthalate tetrahydrate (**5e**) after preparation (**a**) and one full cycle (**b**), both at a magnification of 10,000×.

4. Conclusions

A small library of calcium dicarboxylate salt hydrates was prepared and analyzed with respect to their thermophysical and thermochemical properties to search for potential thermochemical materials. The STA experiments of all candidates showed that these salt hydrates possess promising enthalpies of dehydration. The determined net storage enthalpies correlate to the achievable storage densities, especially highlighting Ca-malonate dihydrate (**2**), Ca-terephthalate trihydrate (**5a**), and Tetrafluoro Ca-terephthalate tetrahydrate (**5e**) as promising candidates, being able to deliver net storage enthalpies at T = 25 °C of 34.59 kJ/mol (**2**), 52.09 kJ/mol (**5a**), and 64.10 kJ/mol (**5e**). The rehydration measurements monitored in situ by PXRD showed effortless rehydration back to the fully hydrated structure. Ca-terephthalate trihydrate indicated full cyclability over the three cycles investigated. In a comparison of SEM images after preparation and after three cycles, no particle degradation could be observed. The absence of the prominent, broad absorption band from 3600 to 2900 cm^{-1} in the IR-spectra of the fully dehydrated salts proves that full dehydration was achieved, and the corresponding diffraction patterns were obtained from the fully dehydrated species. It could be shown that 2-fluoro Ca-terephthalate forms a trihydrate in single crystals and crystallizes in the *Pmna* space group ($Z = 4$, $Z' = \frac{1}{2}$). The crystal is built of infinite chains of Ca atoms located on the *m* 100 reflection plane and connected by 2-fluoroterephthalate ions and water molecules extending in the [100] direction.

To enable a more profound characterization, rehydration measurements on a suitable STA device are to be conducted, ideally resulting in more reliable data on cycle stability. To enable a calculation of the corresponding energy storage densities, density measurements of the salt hydrates are to be performed in the future.

Supplementary Materials: The following supporting information can be downloaded at: https://www.mdpi.com/article/10.3390/cryst13101518/s1, Figure S1: STA of Ca-oxalate monohydrate, Figure S2: STA of Ca-succinate monohydrate, Figure S3: STA of Ca-glutarate monohydrate, Figure S4: STA of 2-methyl Ca-terephthalate n-hydrate, Figure S5: STA of 2-fluoro Ca-terephthalate trihydrate, Figure S6: STA of 2-chloro Ca-terephthalate, measurement 1, Figure S7: STA of 2-chloro Ca-terephthalate, measurement 2, Figure S8: STA of Tetrafluoro Ca-terephthalate tetrahydrate, Figure S9: STA of Tetrachloro Ca-terephthalate n-hydrate, Figure S10: PXRD Ca-oxalate monohydrate, Figure S11: PXRD Ca-oxalate anhydrate, Figure S12: PXRD Ca-malonate dihydrate, Figure S13: PXRD Ca-malonate anhydrate, Figure S14: PXRD Ca-succinate monohydrate, Figure S15: PXRD Ca-succinate anhydrate, Figure S16: PXRD Ca-glutarate monohydrate, Figure S17: PXRD Ca-glutarate anhydrate, Figure S18: PXRD Ca-terephthalate trihydrate, Figure S19: PXRD Ca-terephthalate anhydrate, Figure S20: PXRD 2-fluoro Ca-terephthalate trihydrate, Figure S21: PXRD 2-fluoro Ca-terephthalate anhydrate, Figure S22: PXRD 2-methyl Ca-terephthalate n-hydrate, Figure S23: PXRD 2-methyl Ca-terephthalate anhydrate, Figure S24: FTIR spectrum of Ca-malonate dihydrate, Figure S25: FTIR spectrum of Ca-malonate anhydrate, Figure S26: FTIR spectrum of 2-fluoro Ca-terephthalate trihydrate, Figure S27: FTIR spectrum of 2-fluoro Ca-terephthalate anhydrate, Figure S28: FTIR spectrum of tetrafluoro Ca-terephthalate tetrahydrate, Figure S29: FTIR spectrum of tetrafluoro Ca-terephthalate anhydrate, Table S1: DSC and TG data for Figures 3–9.

Author Contributions: Conceptualization, J.W., J.S. and P.W.; methodology, W.A.; software, W.A.; investigation, J.W. and B.S.; resources, A.W. and P.W.; writing—original draft preparation, J.W. and B.S.; writing—review and editing, J.W., J.S., B.S., A.W. and P.W.; visualization, J.W. and B.S.; supervision, A.W. and P.W.; project administration, A.W.; funding acquisition, A.W. and P.W. All authors have read and agreed to the published version of the manuscript.

Funding: This research was funded by the Austrian Research Promotion Agency (FFG), project number FO999888055.

Data Availability Statement: The data that support the findings of this study are available from the corresponding author upon reasonable request.

Acknowledgments: The authors want to acknowledge the Austrian Research Promotion Agency (FFG) for funding. The X-ray center of TU Wien is acknowledged for their convenient collaboration and for providing access to their devices and facilities. The SEM measurements were carried out using facilities at the University Service Center for Transmission Electron Microscopy, Vienna University of Technology, Austria. We are grateful for their collaboration. Open Access Funding by TU Wien.

Conflicts of Interest: The funders had no role in the design of the study; in the collection, analyses, or interpretation of data; in the writing of the manuscript; or in the decision to publish the results.

References

1. IEA. *Co-Generation and Renewables*; IEA: Paris, Fance, 2011.
2. IEA. *Heating Without Global Warming*; IEA: Paris, France, 2014.
3. Cot-Gores, J.; Castell, A.; Cabeza, L.F. Thermochemical energy storage and conversion: A-state-of-the-art review of the experimental research under practical conditions. *Renew. Sustain. Energy Rev.* **2012**, *16*, 5224. [CrossRef]
4. Dale, S. *BP Statistical Review of World Energy*; BP: London, UK, 2021; p. 60.
5. Knoll, C. Investigations of the Reaction Kinetics of Thermochemical Energy Storage Materials. Ph.D. Thesis, University of Vienna, Vienna, Austria, 2017; p. 200.
6. Hasnain, S.M. Review on sustainable thermal energy storage technologies, Part I: Heat storage materials and techniques. *Energy Convers. Manag.* **1998**, *39*, 1138. [CrossRef]
7. Shine, K.P.; Fuglestvedt, J.S.; Hailemariam, K.; Stuber, N. Alternatives to the Global Warming Potential for Comparing Climate Impacts of Emissions of Greenhouse Gases. *Clim. Chang.* **2005**, *68*, 281–302. [CrossRef]
8. Clark, R.-J.; Mehrabadi, A.; Farid, M. State of the art on salt hydrate thermochemical energy storage systems for use in building applications. *J. Energy Storage* **2020**, *27*, 101145. [CrossRef]
9. Miró, L.; Gasia, J.; Cabeza, L.F. Thermal energy storage (TES) for industrial waste heat (IWH) recovery: A review. *Appl. Energy* **2016**, *179*, 284–301. [CrossRef]
10. Yan, T.; Wang, R.Z.; Li, T.X.; Wang, L.W.; Fred, I.T. A review of promising candidate reactions for chemical heat storage. *Renew. Sustain. Energy Rev.* **2015**, *43*, 13–31. [CrossRef]
11. Ding, Y.; Riffat, S.B. Thermochemical energy storage technologies for building applications: A state-of-the-art review. *Int. J. Low Carbon Technol.* **2013**, *8*, 116. [CrossRef]
12. Donkers, P.A.J.; Sögütoglu, L.C.; Huinink, H.P.; Fischer, H.R.; Adan, O.C.G. A review of salt hydrates for seasonal heat storage in domestic applications. *Appl. Energy* **2017**, *199*, 68. [CrossRef]
13. Hua, W.; Yan, H.; Zhang, X.; Xu, X.; Zhang, L.; Shi, Y. Review of salt hydrates-based thermochemical adsorption thermal storage technologies. *J. Energy Storage* **2022**, *56*, 106158. [CrossRef]
14. Dixit, P.; Reddy, V.J.; Parvate, S.; Balwani, A.; Singh, J.; Maiti, T.K.; Dasari, A.; Chattopadhyay, S. Salt hydrate phase change materials: Current state of art and the road ahead. *J. Energy Storage* **2022**, *51*, 104360. [CrossRef]
15. Du, R.; Wu, M.; Wang, S.; Wu, S.; Wang, R.; Li, T. Experimental investigation on high energy-density and power-density hydrated salt-based thermal energy storage. *Appl. Energy* **2022**, *325*, 119870. [CrossRef]
16. Cabeza, L.F.; Martorell, I.; Miró, L.; Fernández, A.I.; Barreneche, C. *Introduction to Thermal Energy Storage (TES) Systems*; Elsevier Ltd.: Amsterdam, The Netherlands, 2015; p. 28. [CrossRef]
17. Linder, M. Using thermochemical reactions in thermal energy storage systems. In *Advances in Thermal Energy Storage Systems*; Woodhead Publishing: Sawston, UK, 2020; p. 495. [CrossRef]
18. van Essen, V.M.; Cot Gores, J.; Bleijendaal, L.P.J.; Zondag, H.A.; Schuitema, R.; Bakker, M.; van Helden, W.G.J. Characterization of Salt Hydrates for Compact Seasonal Thermochemical Storage. In Proceedings of the ASME 2009 3rd International Conference on Energy Sustainability collocated with the Heat Transfer and InterPACK09 Conferences, San Francisco, CA, USA, 19–23 July 2009; pp. 825–830.
19. Solé, A.; Martorell, I.; Cabeza, L.F. State of the art on gas–solid thermochemical energy storage systems and reactors for building applications. *Renew. Sustain. Energy Rev.* **2015**, *47*, 386–398. [CrossRef]
20. Deutsch, M.; Müller, D.; Aumeyr, C.; Jordan, C.; Gierl-Mayer, C.; Weinberger, P.; Winter, F.; Werner, A. Systematic search algorithm for potential thermochemical energy storage systems. *Appl. Energy* **2016**, *183*, 120. [CrossRef]
21. Knoll, C.; Müller, D.; Artner, W.; Welch, J.M.; Werner, A.; Harasek, M.; Weinberger, P. Probing cycle stability and reversibility in thermochemical energy storage—$CaC_2O_4 \cdot H_2O$ as perfect match? *Appl. Energy* **2017**, *187*, 1–9. [CrossRef]
22. Garofalo, L.; Vitiello, F.V.; Montagnaro, F.; Bürgmayr, H.; Winter, F. Salt Hydrates for Thermochemical Storage of Solar Energy: Modeling the Case Study of Calcium Oxalate Monohydrate Dehydration/Rehydration under Suspension Reactor Conditions. *Ind. Eng. Chem. Res.* **2021**, *60*, 11357–11372. [CrossRef]
23. Kazuo, M. Thermal behavior of alkaline earth metal malonate hydrates and their anhydrides. *Thermochim. Acta* **1996**, *286*, 198. [CrossRef]

24. Galwey, A.K.; Abdel Aziz Mohamed, M. Thermal decomposition of calcium malonate dihydrate. *Solid State Ion.* **1990**, *42*, 135–145. [CrossRef]
25. Brusau, E.V.; Narda, G.E.; Pedregosa, J.C.; Varetti, E.L. A low temperature infrared study of the coordinated water in calcium malonate dihydrate. *Spectrochim. Acta A Mol. Biomol. Spectrosc.* **2002**, *58*, 1769–1774. [CrossRef]
26. Christy, D.S.; Mahadevan, C.K.; Shajan, X.S. Growth by free evaporation method and physico—Chemical properties of calcium succinate single crystals. *Optik* **2017**, *145*, 418–427. [CrossRef]
27. Binitha, M.P.; Pradyumnan, P.P. Studies on growth, thermal and dielectric behavior of calcium succinate trihydrate single crystals. *J. Cryst. Growth* **2014**, *396*, 44. [CrossRef]
28. Li, Y.; Yi, H.; Ge, M.; Yao, D. Scale-Up Synthesis of High Purity Calcium Terephthalate from Polyethylene Terephthalate Waste: Purification, Characterization, and Quantification. *Macromol. Mater. Eng.* **2021**, *306*, 2100591. [CrossRef]
29. Mazaj, M.; Mali, G.; Rangus, M.; Žunkovič, E.; Kaučič, V.; Zabukovec Logar, N. Spectroscopic Studies of Structural Dynamics Induced by Heating and Hydration: A Case of Calcium-Terephthalate Metal–Organic Framework. *J. Phys. Chem. C* **2013**, *117*, 7552–7564. [CrossRef]
30. Groeneman, R.H.; Atwood, J.L. Terephthlate bridged coordination polymers based upon group two metals. *Cryst. Eng.* **1999**, *2*, 249. [CrossRef]
31. Dominici, F.; Sarasini, F.; Luzi, F.; Torre, L.; Puglia, D. Thermomechanical and morphological properties of poly(ethylene terephthalate)/anhydrous calcium terephthalate nanocomposites. *Polymers* **2020**, *12*, 276. [CrossRef]
32. Zolgharnein, J.; Dermanaki Farahani, S. Experimental design optimization and isotherm modeling for removal of copper(II) by calcium-terephthalate MOF synthesized from recycled PET waste. *J. Chemom.* **2023**, *37*, e3396. [CrossRef]
33. Mazaj, M.; Zabukovec Logar, N. Phase Formation Study of Ca-Terephthalate MOF-Type Materials. *Cryst. Growth Des.* **2015**, *15*, 617–624. [CrossRef]
34. Matsuzaki, T.; Iitaka, Y. The crystal structure of calcium terephthalate trihydrate. *Acta Crystallogr. Sect. B* **1972**, *28*, 1977–1981. [CrossRef]
35. Barsk, A.; Yazdani, M.R.; Kankkunen, A.; Seppälä, A. Exceptionally high energy storage density for seasonal thermochemical energy storage by encapsulation of calcium chloride into hydrophobic nanosilica capsules. *Sol. Energy Mater. Sol. Cells* **2023**, *251*, 112154. [CrossRef]
36. Donkers, P.A.J.; Adan, O.C.G.; Smeulders, D.M.J. Hydration/Dehydration Processes in Stabilized $CaCl_2$. In *Poromechanics VI*; American Society of Civil Engineers: Reston, VA, USA, 2017; pp. 656–663. [CrossRef]
37. Donkers, P.A.J.; Beckert, S.; Pel, L.; Stallmach, F.; Steiger, M.; Adan, O.C.G. Water Transport in $MgSO_4 \cdot 7H_2O$ During Dehydration in View of Thermal Storage. *J. Phys. Chem. C* **2015**, *119*, 28711–28720. [CrossRef]
38. Van Essen, V.; Zondag, H.; Gores, J.C.; Bleijendaal, L.; Bakker, M.; Schuitema, R.; Van Helden, W.; He, Z.; Rindt, C. Characterization of $MgSO_4$ hydrate for thermochemical seasonal heat storage. *J. Sol. Energy Eng.* **2009**, *131*, 041014. [CrossRef]
39. Whiting, G.; Grondin, D.; Bennici, S.; Auroux, A. Heats of water sorption studies on zeolite–$MgSO_4$ composites as potential thermochemical heat storage materials. *Sol. Energy Mater. Sol. Cells* **2013**, *112*, 112–119. [CrossRef]
40. Ferchaud, C.; Zondag, H.; Veldhuis, J.; De Boer, R. Study of the reversible water vapour sorption process of $MgSO_4.7H_2O$ and $MgCl_2.6H_2O$ under the conditions of seasonal solar heat storage. *J. Phys. Conf. Ser.* **2012**, *395*, 012069. [CrossRef]
41. Clark, R.-J.; Farid, M. Hydration reaction kinetics of $SrCl_2$ and $SrCl_2$-cement composite material for thermochemical energy storage. *Sol. Energy Mater. Sol. Cells* **2021**, *231*, 111311. [CrossRef]
42. Blijlevens, M.A.R.; Mazur, N.; Kooijman, W.; Fischer, H.R.; Huinink, H.P.; Meekes, H.; Vlieg, E. A study of the hydration and dehydration transitions of $SrCl_2$ hydrates for use in heat storage. *Sol. Energy Mater. Sol. Cells* **2022**, *242*, 111770. [CrossRef]
43. Al-Terkawi, A.-A.; Scholz, G.; Prinz, C.; Zimathies, A.; Emmerling, F.; Kemnitz, E. Hydrated and dehydrated Ca-coordination polymers based on benzene-dicarboxylates: Mechanochemical synthesis, structure refinement, and spectroscopic characterization. Electronic supplementary information (ESI) available: Powder X-ray diffraction data, ATR-infrared spectra, EXAFS spectra, EXAFS data, SEM images, adsorption isotherms, and crystal data. CCDC Four files containing the crystal parameters of compounds 1 (CCDC 1582672), (1-H2O) (CCDC 1582673), 2 (CCDC 1582675), and 3 (CCDC 1582674). *CrystEngComm.* **2018**, *20*, 946–961. [CrossRef]
44. *X-Area 1.31.175.0, LANA 2.6.2.0*; STOE & Cie GmbH: Darmstadt, Germany, 2021.
45. Sheldrick, G. SHELXT—Integrated space-group and crystal-structure determination. *Acta Crystallogr. Sect. A* **2015**, *71*, 3–8. [CrossRef] [PubMed]
46. Petříček, V.; Dušek, M.; Palatinus, L. Crystallographic Computing System JANA2006: General features. *Z. Für Krist.-Cryst. Mater.* **2014**, *229*, 345–352. [CrossRef]
47. Macrae, C.F.; Edgington, P.R.; McCabe, P.; Pidcock, E.; Shields, G.P.; Taylor, R.; Towler, M.; van de Streek, J. Mercury: Visualization and analysis of crystal structures. *J. Appl. Crystallogr.* **2006**, *39*, 453–457. [CrossRef]
48. Ben Chanaa, M.b.; Lallemant, M.; Bertrand, G. Exploration systematique de la cinetique de rehydratation d'un sel renversable. Exemple de la reaction $CaC_2O_4(s) + H_2O(g) \rightarrow CaC_2O_4 \cdot H_2O(s)$. *Thermochim. Acta* **1986**, *97*, 369–385. [CrossRef]
49. Gaisford, S.; Kett, V.; Haines, P. *Principles of Thermal Analysis and Calorimetry*, 2nd ed.; Royal Society of Chemistry: Cambridge, UK, 2016.

50. N'Tsoukpoe, K.E.; Schmidt, T.; Rammelberg, H.U.; Watts, B.A.; Ruck, W.K.L. A systematic multi-step screening of numerous salt hydrates for low temperature thermochemical energy storage. *Appl. Energy* **2014**, *124*, 1–16. [CrossRef]
51. Dornberger-Schiff, K.; Grell-Niemann, H. On the theory of order-disorder (OD) structures. *Acta Crystallogr.* **1961**, *14*, 167–177. [CrossRef]